An optimal approach to overlapping bands with correlated *k* distribution method and its application to radiative calculations

Hua Zhang,[1,2] Teruyuki Nakajima,[3] Guangyu Shi,[4] Tsuneaki Suzuki,[1] and Ryoichi Imasu[3]

Received 25 December 2002; revised 9 June 2003; accepted 19 June 2003; published 25 October 2003.

[1] It is found that the possibly achieved higher accuracy cannot be obtained for all overlapping bands if only one scheme is used to treat them in atmospheric absorption calculations. The commonly used multiplication transmittance scheme is not acceptable when correlation existing in the practical absorption spectra becomes strong. Therefore an optimized scheme to obtain *k* distribution parameters for overlapping bands is developed in this paper based on the completely uncorrelated, perfectly correlated, and partly correlated schemes. Two partial correlation formulae are given in the paper. Calculations of radiative flux and atmospheric heating (or cooling) rate are validated in detail using a line-by-line model described in the paper for six model atmospheres. The optimized scheme developed here has an accuracy in longwave clear skies of 0.07 K d^{-1} in the entire troposphere and 0.35 K d^{-1} above the tropopause; the accuracy of upward, downward, and net fluxes is 0.76 W m^{-2} at all altitudes. In shortwave region, the absolute errors of the heating rate are less than 0.05 K d^{-1} in the troposphere and less than 0.25 K d^{-1} above the tropopause; net flux errors are less than 0.9 W m^{-2} at all altitudes. For an ensemble of 42 diverse atmospheres, the new scheme guarantees an average maximum error of longwave heating rate of 0.068 K d^{-1} in troposphere, 0.22 K d^{-1} above tropopause, and an accuracy of 1.1 W m^{-2} of radiative net flux for all the levels. For a case of doubled CO_2 concentration, radiative forcing calculations have an accuracy of 0.04 W m^{-2}. *INDEX TERMS:* 0360 Atmospheric Composition and Structure: Transmission and scattering of radiation; 1610 Global Change: Atmosphere (0315, 0325); 3359 Meteorology and Atmospheric Dynamics: Radiative processes; *KEYWORDS:* atmospheric absorption, correlated *k* distribution, overlapping band

Citation: Zhang, H., T. Nakajima, G. Shi, T. Suzuki, and R. Imasu, An optimal approach to overlapping bands with correlated *k* distribution method and its application to radiative calculations, *J. Geophys. Res.*, *108*(D20), 4641, doi:10.1029/2002JD003358, 2003.

1. Introduction

[2] Many techniques are available to model atmospheric absorption of radiation by greenhouse gases. Line-by-line (LBL) procedures are the most precise schemes, but as they are not practical to apply because of the cost of integration over all wavelengths they usually serve as a reference for other models. Correlated *k* distribution (henceforth ck-D) methods simplify wavelength integration by resorting the absorption spectrum, greatly reducing the calculation time yet retaining high accuracy.

[3] The method by which overlapping absorption bands are treated affects the accuracy and speed of radiative transfer calculations in the ck-D approach. Numerous overlapping bands exist in the atmosphere, i.e., bands in which different gases absorb at the same wavelengths. For example, both CH_4 and N_2O absorb at 7–8 μm; CO_2, H_2O, and O_3 at 15 μm, and CO_2 and H_2O at 2.7 μm, and so on.

[4] Several methods have been proposed to deal with this effect. One method combines two or more overlapping line absorbers to generate a "single complex gas," i.e., a single representative absorption spectrum to two or more line absorbers [*Goody et al.*, 1989; *Fu and Liou*, 1992; *Mlawer et al.*, 1997]. However, this method is not appropriate for some remote sensing applications that require the individual *k* distribution functions of each gas to be defined separately [*Buchwitz et al.*, 2000]. Moreover, the selection of the principal absorber requires limiting the range of mixing ratios for gases [*Gerstell*, 1993].

[5] The second widely adopted method combines absorption coefficients determined individually for each absorber by assuming a spectral correlation between the absorption spectra for overlapping gases [*Shi*, 1981; *Isaacs et al.*, 1987; *Lacis and Oinas*, 1991; *Firsov et al.*, 1998]. The most common approach is to assume that the monochromatic transmittances or absorption spectra of the overlapping line absorbers are uncorrelated within the wavelength interval of interest [*Wang and Ryan*, 1983; *Lacis and Oinas*, 1991; *Ellingson et al.*, 1991]. The mean transmittance for such a

[1]Integrated Modeling Research Program, Frontier Research System for Global Change, Yokohama, Japan.
[2]Now at Dynamical Climate Division, National Climate Center, China Meteorological Administration, Beijing, China.
[3]Center for Climate System Research, University of Tokyo, Tokyo, Japan.
[4]State Key Laboratory of Numerical Modeling for Atmospheric Sciences and Geophysical Fluid Dynamics, Institute of Atmospheric Physics, Beijing, China.

0148-0227/03/2002JD003358$09.00

case can be calculated as the product of the mean transmittances of the individual absorber. The radiative transfer equation then must be solved M^2 times (M is the number of discrete quadrature points of wavelength integration) with a combination of absorption coefficients $\{k_i^1 \times k_j^2;\ i, j = 1, \ldots, M\}$, for example, in a two-overlapping-gas case. Such treatment is reasonably accurate for finite but small spectral intervals like the narrowband model. Ignoring the correlation between the line absorption of overlapping gases may yield noticeable errors. Another scheme under the ck-D framework assumes that the absorption spectra of gases are perfectly correlated [*Isaacs et al.*, 1987; *Liu et al.*, 2001]. For this scheme, the shape of the absorption coefficient distribution is assumed to be the same. Thus only the magnitude can be different, so only coefficients with the same quadrature index $\{k_i^1 \times k_j^2;\ i, j = 1, \ldots, M\}$ need to be combined, and M-radiative transfer calculations are necessary in this scheme. The underlying correlation assumption, however, is unrealistic and yields a significant systematic overestimation of transmittance in most cases [*Shi*, 1981, 1984; *Firsov et al.*, 1998]. A third scheme that accounts for partial correlation between the line absorbers is worth exploring.

[6] *Shi* [1981] proposed several approaches to treat atmospheric overlapping bands with k distribution method based on the relative intensities of overlapping gases and the correlation among them. However, he only gave the transmittance differences caused by the different treatments for a homogeneous atmospheric path and did not tell us which one is the best for an inhomogeneous path. *Liu et al.* [2001] compared several schemes that did not include the partial correlation. Some past works have considered partial correlations, but these works used only a multiplying transmittance scheme as the reference criteria and did not compare results with those of the most accurate LBL models [*Shi*, 1984; *Liu et al.*, 2001]. *Yang et al.* [2000] proposed several approaches to modify traditional methods [*Fu and Liou*, 1992; *Lacis and Oinas*, 1991] with including partial correlations, but they are only for remote sensing with very narrow bandwidths. In contrast to the above methods, *Nakajima et al.* [2000] developed a nonlinear optimizing successive-quadrature program (SQP) that automatically tunes the k distribution coefficients to account for partial correlations.

[7] Previous research has shown that there is no universal treatment appropriate to all overlapping bands or channels for use in climate or remote sensing study because the correlation varies widely among overlapping bands. Even the method of *Nakajima et al.* [2000] includes poorly convergent cases to obtain k distribution function. Thus it will be useful to develop a more objective method to find k distribution parameters by combining several correlation methods.

[8] The present study gives two simplified schemes on partial correlation that include the correlation between different gas absorption spectra by mapping the absorption spectrum of the second or third gas to that of the primary gas [e.g., *Shi*, 1981, 1984; *Mlawer et al.*, 1997]. Then, the correlation existing between the overlapping gases is automatically contained in the calculated transmittance and radiative flux; special solving as by *Firsov et al.* [1998] is unnecessary. Therefore the optimal scheme is proposed in this study that chooses k distribution parameters for overlapping bands based on the completely uncorrelated, perfectly correlated, and partly correlated schemes, as described above. The performance of the new approach for overlapping bands has been confirmed, as shown in section 4.

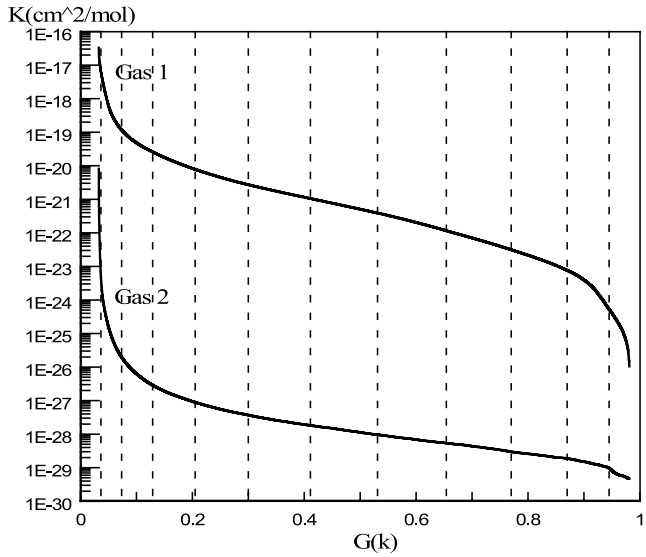

Figure 1. Schematic of resorting method for completely uncorrelated and perfectly correlated transmission model. The abscissa represented by $G(k)$ is the cumulative k distribution [e.g., see *Lacis and Oinas*, 1991]; the ordinate represents the absorption coefficient. Dashed lines in the figure show the position of Gaussian quadrature points [e.g., see *Shi*, 1981].

[9] Section 2 describes several transmission schemes used in the present optimal method. Section 3 introduces algorithms of the absorption coefficients and effective absorption coefficients and radiative transfer scheme used in the LBL model and ck-D approach; validations in sections 4 and 5 provide a summary.

2. Transmission Schemes for Overlapping Bands With a ck-D Method

[10] How can the combined transmission of two gaseous absorbers be solved if the two gases (1 and 2) overlap in a spectral band? Two overlapping schemes are available if we resort each gas in an overlapping band independently (see Figure 1) and adopt the ck-D hypothesis [*Zhang and Shi*, 2002] for vertically inhomogeneous atmosphere for each gas. One is the commonly used multiplying transmission method which assumes that the absorption spectrum between overlapping gases is completely uncorrelated, in which the multiple transmission is expressed with ck-D as

$$T(u_1, u_2) = T(u_1)T(u_2) = \sum_{\substack{i=1,M \\ j=1,N}} A_i A_j \exp\left[-\left(k_i^1 u_1 + k_j^2 u_2\right)\right]. \quad (1)$$

Here u_1 and u_2 are the absorption amounts of two gases, $\{k_i^1,\ i = 1,\ M\}$ and $\{k_j^2,\ j = 1,\ N\}$ are the equivalent absorption coefficients at Gaussian quadrature points (or

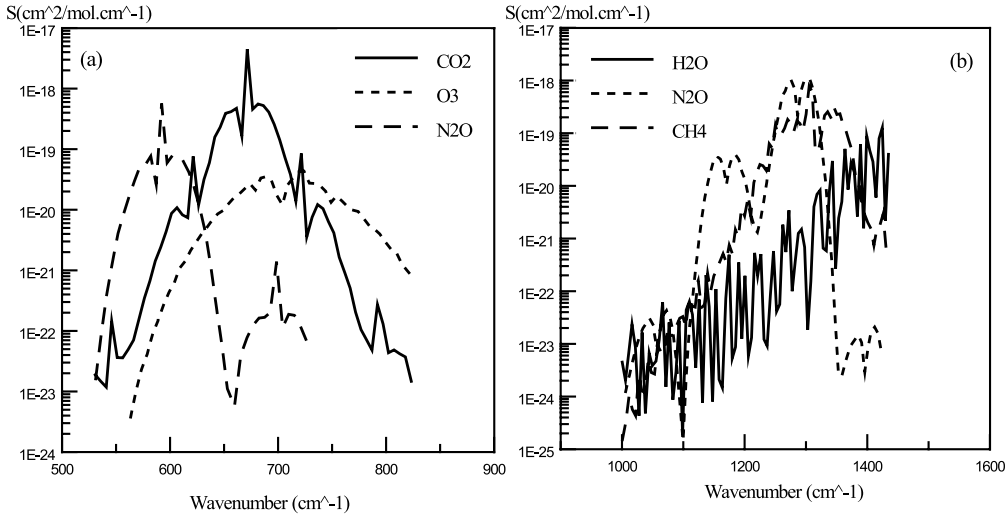

Figure 2. Schematic illustration of correlation among radiative gases of two typical overlapping bands. (a) CO_2, O_3, and N_2O 15 μm band. (b) H_2O, N_2O, and CH_4 7.8 μm band. The abscissa is wave number; the ordinate represents the mean line strength of absorptive gas within every 5 cm^{-1}.

subintervals) for gas 1 and gas 2, respectively. Superscripts of k_i^1 and k_j^2 denote the gas species; M and N are the total numbers of subintervals for gas 1 and gas 2, respectively. A_i and A_j are the correspondent Gaussian quadrature weights for gas 1 and gas 2.

[11] The second scheme is the so-called perfectly correlated scheme. The formula for the overlapping transmission in this scheme is

$$T(u_1, u_2) = \sum_{i=1}^{M} A_i \exp\left[\left(k_i^1 u_1 + k_i^2 u_2\right)\right]. \tag{2}$$

The meanings of A_i, u_1, u_2, and M here are all the same as those of formula (1). The difference between formulae (1) and (2) is the inclusion in formula (1) of cross-product terms of the two gases because of the random hypothesis of absorption spectra. Formula (2) does not contain such terms because the two absorption spectra are assumed to be perfectly correlated.

[12] Formula (1) yields an accurate overlapping transmittance of two or more gases when it is used in a wave number integration with LBL or in a narrowband scheme with a bandwidth less than several tens of wave number. It may underestimate or overestimate the overlapping transmittance when the correlation among gases becomes strong [*Shi*, 1984; *Chou et al.*, 2001]. Formula (2) overestimates the overlapping transmission in most cases [*Firsov et al.*, 1998] because the hypothesis of perfect correlation is rarely satisfied in the real absorption spectrum.

[13] Figures 2a and 2b show the average absorption spectra for wave number ranges 550–850 and 1000–1450 cm^{-1}, which are two typical overlapping bands in the atmosphere, i.e., the 15 μm band for CO_2, O_3, and N_2O, and the 7.8 μm band for H_2O, CH_4, and N_2O. Similar wave number dependences of the averaged absorption of the three gases in Figures 2a and 2b suggest that there must be a significant correlation among the absorbers. On the basis of this, a suitable approximation between formulae (1) and (2) is given next, which considers the partial correlation existing among different gas absorption spectra.

[14] Figure 3 schematically illustrates the present scheme for partly correlated overlapping bands. First, a reference gas is chosen among the considered gas species according to the product of the integrated line strength and its abundance in each band. This product effectively indicates the level of radiative importance of the species within every divided band [*Mlawer et al.*, 1997]. In other words, let ξ represent the product,

$$\xi = SW, \tag{3}$$

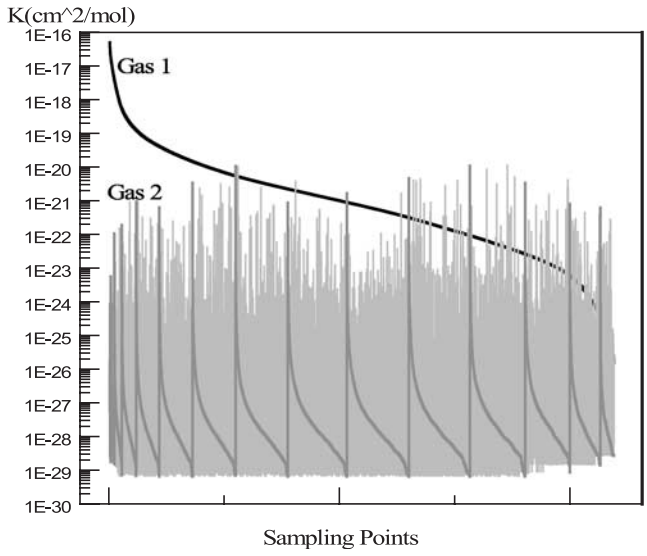

Figure 3. Schematic of the approach for overlapping band with partial correlation assumption. The solid line represents the sorted curve of reference gas (gas 1), while the pale shaded line is the mapping of nonreference gas (gas 2) to gas 1; shaded lines represent the secondary resorted absorption coefficients of gas 2 at each subinterval. The ordinate in the figure is the same as in Figure 1, while the abscissa is the sampling points.

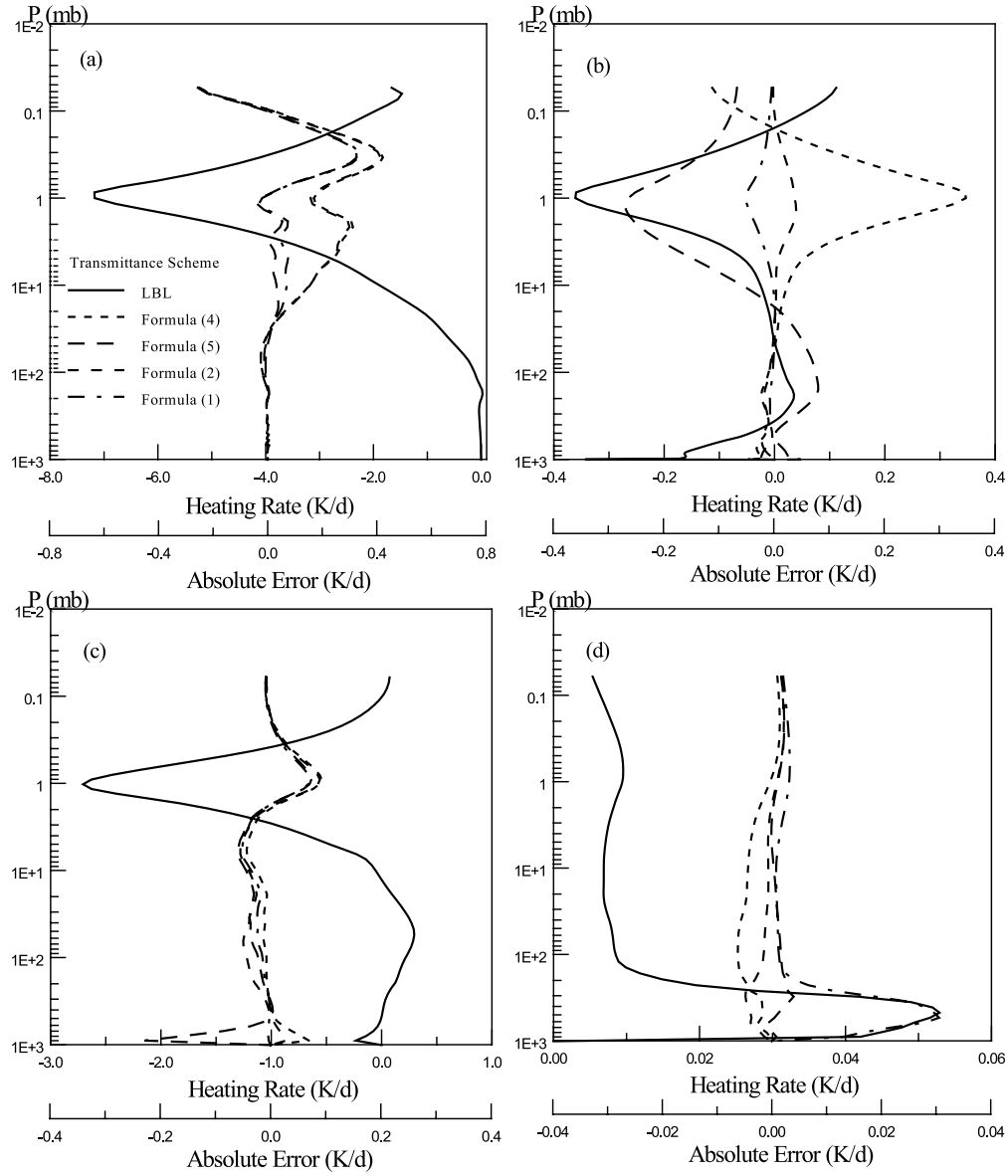

Figure 4. The comparison of heating rates for four transmission schemes to those of LBL model. (a) H_2O, CO_2, and O_3 (630–700 cm^{-1}). (b) H_2O, N_2O, and CH_4 (1200–1350 cm^{-1}). (c) H_2O, CO_2, and O_3 (940–1200 cm^{-1}). (d) H_2O and CH_4 (3900–4540 cm^{-1}).The solid line represents LBL results; different dashed lines represent errors of the four schemes to LBL results.

where S and W are the integrated line strength and integrated column amount of each species, respectively. The gas with the biggest ξ value at each band is considered as the reference gas, like gas 1 in Figure 3, for example. We adopt the ck-D hypothesis for the reference gas, namely, the biggest absorption coefficients at one pressure or/and temperature correspond to the biggest at another pressure or/and temperature [*Zhang and Shi*, 2002]. However, we do not make such a hypothesis for nonreference gases such as gas 2 in Figure 3 or a third gas if there is three-gas overlapping. Instead, we remap their absorption coefficients at the given pressures and temperatures according to the position of that of the reference gas at a reference pressure and temperature in the process of sorting the absorption spectrum of the reference gas. The optimal reference pressure and temperature, found by trial and error, are 1 mbar and 260 K for all bands. Therefore the correlation information of gas 2 is kept in the remapped spectrum. There are two ways to treat the remapped spectrum of gas 2 and therefore two algorithms to obtain the effective absorption coefficient at each subinterval of the second absorber. One is to reorder the absorption coefficients of gas 2 at each subinterval again to produce a smooth curve (gray lines in Figure 3) and then to calculate a median value around each Gaussian quadrature point to derive the effective absorption coefficient k_i^2. The overlapped transmittance then becomes

$$T(u_1, u_2) = \sum_{i=1}^{M} A_i \exp\left[-\left(k_i^1 u_1 + k_i^2 u_2\right)\right]. \quad (4)$$

Note that although formulae (2) and (4) are similar, the algorithm to solve the effective absorption coefficients k_i^1

and k_i^2 is different. If we use the average of all the absorption coefficients to produce the effective absorption coefficient $\overline{k_i^2}$ at each subinterval (see section 3 for the detailed algorithm to obtain k_i^2 and $\overline{k_i^2}$), then we obtain the second formula to calculate the overlapped transmittance for partial correlation

$$T(u_1, u_2) = \sum_{i=1}^{M} A_i \exp\left[-\left(k_i^1 u_1 + \overline{k_i^2} u_2\right)\right]. \quad (5)$$

The meanings of A_i, u_1, u_2, and M in formulae (4) and (5) are the same as those in formula (1). We use both formulae to select the final k distribution parameters in the optimal method for calculation accuracy. We should point out that formulae (4) and (5) are developed after equation (3) of *Shi* [1984], but they have the same accuracy as the above equation and faster speed than it as we test. Because equation (3) of *Shi* [1984] gave more detailed divisions at each subinterval for minor gases, it makes the speed of overlapped transmittance calculation become slower than formulae (2), (3), (4), and also formula (1) in this work. Therefore equation (3) of *Shi* [1984] is not included in the discussions of this optimal method. However, it may be useful to very narrowband studies for some remote sensing application that is beyond of the scope of this study.

[15] Figures 4a–4d show the heating rate for the overlapping bands at 15 μm (630–700 cm^{-1}; H_2O, CO_2, and O_3), 7.8 μm (1200–1350 cm^{-1}; H_2O, CH_4, and N_2O), 9.6 μm (940–1200 cm^{-1}; H_2O, CO_2, and O_3) and 2.5 μm (3900–4540 cm^{-1}; H_2O and CH_4) from the LBL integration, compared to heating rates calculated by the four ck-D transmittance models, given by formulae (1), (2), (4), and (5). Formula (1) yields the best approximation for the 7.8 and 9.6 μm overlapping bands, while formula (5) is the best at 15 and 2.5 μm. In other words, using only one of the completely correlated, perfectly correlated, and partly correlated schemes will not ensure accuracy. Physically speaking, the correlation in each band varies from almost completely uncorrelated to almost perfectly correlated; most cases, however, are partly correlated. This correlation behavior suggests that all four schemes should be included in the calculations. It should be noted here that how to obtain effective absorption coefficient in the four transmittance schemes is another important factor to decide the final accuracy in each subinterval of each overlapping band as we see in section 3.

[16] We adopt a criterion to choose a priori the best method before detailed k distribution calculations,

$$\mathrm{Diff} = \frac{1}{M_{\mathrm{layer}} N_{\mathrm{atm}}} \sum_{\substack{\mathrm{layer}=1 \\ i\mathrm{atm}=1}}^{\substack{N_{\mathrm{atm}} \\ M_{\mathrm{layer}}}} \left(\mathrm{CR}_{\substack{\mathrm{layer} \\ i\mathrm{atm}}}^{\mathrm{ck-D}} - \mathrm{CR}_{\substack{\mathrm{layer} \\ i\mathrm{atm}}}^{\mathrm{LBL}} \right)^2, \quad (6)$$

where N_{atm} and M_{layer} represent the number of model atmospheres and vertical layers, taken to be 6 and 75, respectively, in the present work. Vertical resolution of the atmosphere is 1 km. Formula (6) is a score function related to RMS error of atmospheric heating (or cooling) rates (denoted by CR) of ck-D to LBL integration for six model atmospheres. Diff is the criterion in the optimizing calculation. We choose the optimal scheme with the minimum Diff value among the four schemes for the practical calculation.

Table 1. Band Configuration

Band	Wave Number, cm^{-1}	k Interval	Gases	Transmittance Model
1	10–250	12	H_2O	
2	250–430	14	H_2O	
3	430–530	16	H_2O	
4	530–630	14	H_2O, CO_2, N_2O	formula (1)
5	630–700	16	H_2O, CO_2, O_3	formula (5)
6	700–820	16	H_2O, CO_2, O_3	formula (1)
7	820–940	6	H_2O	
8	940–1200	10	H_2O, CO_2, O_3	formula (1)
9	1200–1300	9	H_2O, CH_4	formula (4)
10	1300–1390	14	H_2O, N_2O, CH_4	formula (1)
11	1390–1480	16	H_2O	
12	1480–1810	14	H_2O	
13	1810–2110	10	H_2O	
14	2110–2680	14	H_2O, CO_2, N_2O	formula (1)
15	2680–3500	8	H_2O, CH_4	formula (2)
16	3500–3900	15	H_2O, CO_2	formula (2)
17	3900–4540	16	H_2O, CH_4	formula (5)
18	4540–6150	16	H_2O	
19	6150–8050	15	H_2O	
20	8050–12,000	16	H_2O	
21	12,000–22,000	3	H_2O, O_3	formula (5)
22	22,000–31,000			
23	31,000–33,000	2	O_3	
24	33,000–35,000	2	O_3	
25	35,000–37,000	2	O_3	
26	37,000–43,000	4	O_3, O_2	formula (1)
27	43,000–49,000	2	O_3, O_2	formula (5)

3. Computational Scheme

[17] The detailed algorithm in this work is described in the following. The HITRAN'2000 database (L. S. Rothman et al., The HITRAN molecular spectroscopic database and HAWKS (HITRAN Atmospheric Workstation), 2000, available at http://www.hitran.com) is used to give line parameters and cross sections. CKD_2.4 (S. A. Clough et al., 2000, available at http://www.rtweb.aer.com) generates continuum absorption coefficients due to water vapor, CO_2, O_3, and O_2. Absorption coefficients at 22 pressure levels and 3 temperatures (200, 260, and 320 K) that range over the entire atmosphere are computed by LBLRTM (S. A. Clough et al., 2000, available at http://www.rtweb.aer.com) with a spectral interval of 1/4 of the mean spectral line half-width and with a 25-cm^{-1} cutoff for line wings over each band [*Clough et al.*, 1992; *Clough and Iacono*, 1995]. The 22 pressure levels are from the AFGL midlatitude summer (MLS) atmospheric pressure profile and include 0.01, 0.0158, 0.0215, 0.0251, 0.0464, 0.1, 0.158, 0.215, 0.398, 0.464, 1.0, 2.15, 4.64, 10.0, 21.5, 46.4, 100.0, 220.0, 340.0, 460.0, 700.0, and 1013.25 mbar.

[18] Many approaches account for the variation of absorption coefficients with pressure, including the fitting method [*Shi*, 1981; *Nakajima et al.*, 2000], the scaling approximation method [*Chou*, 1999; *Chou et al.*, 2001], and the interpolation method [*Mlawer et al.*, 1997]. The interpolation scheme is the most accurate according to our detailed tests, so it is used in this study with linear

Table 2. Comparison of Effects on Fluxes Due to Doubled CO_2 Concentration From 355 ppmv Among the LBL Model, ck-D Model, and LBLRTM[a]

		TOA Net Flux		Tropopause						Surface Net Flux	
Band Number	Wave Number Range, cm^{-1}	LBL	CKD	LBL Upward Flux	CKD Upward Flux	LBL Downward Flux	CKD Downward Flux	LBL Net Flux	CKD Net Flux	LBL	CKD
4	530–630	−1.04	−1.04	−1.08	−1.07	0.68	0.69	−1.75	−1.76	−0.03	−0.04
5	630–700	0.61	0.60	−0.32	−0.32	0.35	0.35	−0.68	−0.67	0.00	0.00
6	700–820	−1.66	−1.67	−1.83	−1.80	0.60	0.56	−2.43	−2.36	−0.89	−0.89
8	940–1200	−0.33	−0.34	−0.36	−0.37	0.01	0.01	−0.37	−0.38	−0.66	−0.67
14	2110–2680	−0.03	−0.04	−0.04	−0.05	0.00	0.00	−0.04	−0.06	−0.03	−0.05
Total	10–2680	−2.45	−2.49	−3.63	−3.61	1.64	1.61	−5.27	−5.23	−1.61	−1.65
Error 1		0.04	0.04	0.02	0.02	0.03	0.03	0.04	0.04	0.04	0.04
Error 2		0.39	0.35	0.25	0.27	0.06	0.09	0.31	0.35	0.20	0.16
Reference		LBLRTM		LBLRTM		LBLRTM		LBLRTM		LBLRTM	
	10–3000	−2.84		−3.88		1.70		−5.58		−1.81	

[a]The listed bands are only those including CO_2 gas in the thermal region. Error 1 in the table is the difference between ck-D model and LBL model; error 2 is the difference between our LBL model and LBLRTM and our ck-D model and LBLRTM. The reference values of LBLRTM are taken from the work of *Mlawer et al.* [1997]. All the difference values in the table represent the absolute values. Units of all fluxes are in W m^{-2}.

interpolation on the pressure axis and formula (7) on the temperature axis [*Shi*, 1998; *Zhang*, 1999], as below,

$$k = k_0 \left(\frac{T}{T_0}\right)^{(a+bT)}, \tag{7}$$

where k_0 is the absorption coefficient at a reference temperature T_0 of 260 K; a and b are functions of pressure. Please see the work of *Zhang* [1999] for the detailed algorithm on a and b in formula (7). In this way, the absorption coefficient at any layer can be obtained.

[19] We now describe the detailed algorithm to obtain effective absorption coefficient k_i including k_i^1, k_i^2, and $\overline{k_i^2}$ in the four-transmittance models given by formulae (1), (2), (4), and (5) in section 2. The absorption coefficients for a reference gas are sorted in descending order as by *Shi* [1981] at the 22 pressures and 3 temperatures noted above. The effective absorption coefficients for the reference gas, i.e., k_i^1 in formulae (1), (2), (4), and (5), can be derived by two methods. Method 1 includes averages of all the $k(g)$ values [see *Lacis and Oinas*, 1991] in each subinterval of the reference gas. Method 2 averages the $k(g)$ values in the narrow range near every Gaussian quadrature point. In method 1, larger $k(g)$ values dominate in each subinterval because of the arithmetic mean. Usually, there exists 5–10 orders of magnitude difference in absorption coefficients at each subinterval so that the arithmetic mean results in only considering the bigger absorption coefficients at the subinterval. This becomes one error source to produce effective absorption coefficient. Although method 1 yields accurate heating rates between 66 km and the top of the atmosphere (TOA), results in the stratosphere and middle atmosphere below 66 km become inaccurate. In method 2, the median k_i value dominates in each subinterval that make heating rates in the stratosphere and middle atmosphere below 66 km become more accurate because the median values of k_i are effective at these altitudes, while the largest values of k_i affect the heating rates above 66 km [*Mlawer et al.*, 1997; *Zhang*, 1999]. We use method 2 to solve k_i^1 for the reference gas in the following calculations because the TOA in most atmospheric general circulation models (AGCMs) is below 66 km.

[20] Two schemes are available for minor gases to produce effective absorption coefficient at each subinterval.

Table 3. Comparison of Net Flux for Six Atmospheres at Solar and Thermal Region

		TOA, W m^{-2}		Tropopause, W m^{-2}		Surface, W m^{-2}	
Atmosphere	Region	Net Flux[a]	Difference[b]	Net Flux	Difference	Net Flux	Difference
TRO	LW	280.89	0.66	270.58	0.36	62.13	0.46
	SW	565.00	0.21	541.78	0.19	412.14	0.48
MLS	LW	275.64	0.53	258.86	0.27	76.05	0.00
	SW	563.03	0.24	536.82	0.30	418.86	0.51
MLW	LW	227.64	0.19	216.13	0.22	89.06	0.50
	SW	554.95	0.19	532.33	0.16	443.76	0.61
SAS	LW	259.33	0.41	230.22	0.20	85.88	0.24
	SW	560.55	0.23	531.10	0.56	426.59	0.48
SAW	LW	197.08	0.05	190.70	0.00	78.37	0.66
	SW	550.64	0.22	535.52	0.16	456.30	0.69
USS	LW	256.34	0.41	235.18	0.08	104.97	0.01
	SW	557.87	0.21	528.82	0.55	434.66	0.49

[a]Represents the LBL result.
[b]Absolute difference of net flux between the ck-D model and LBL model.

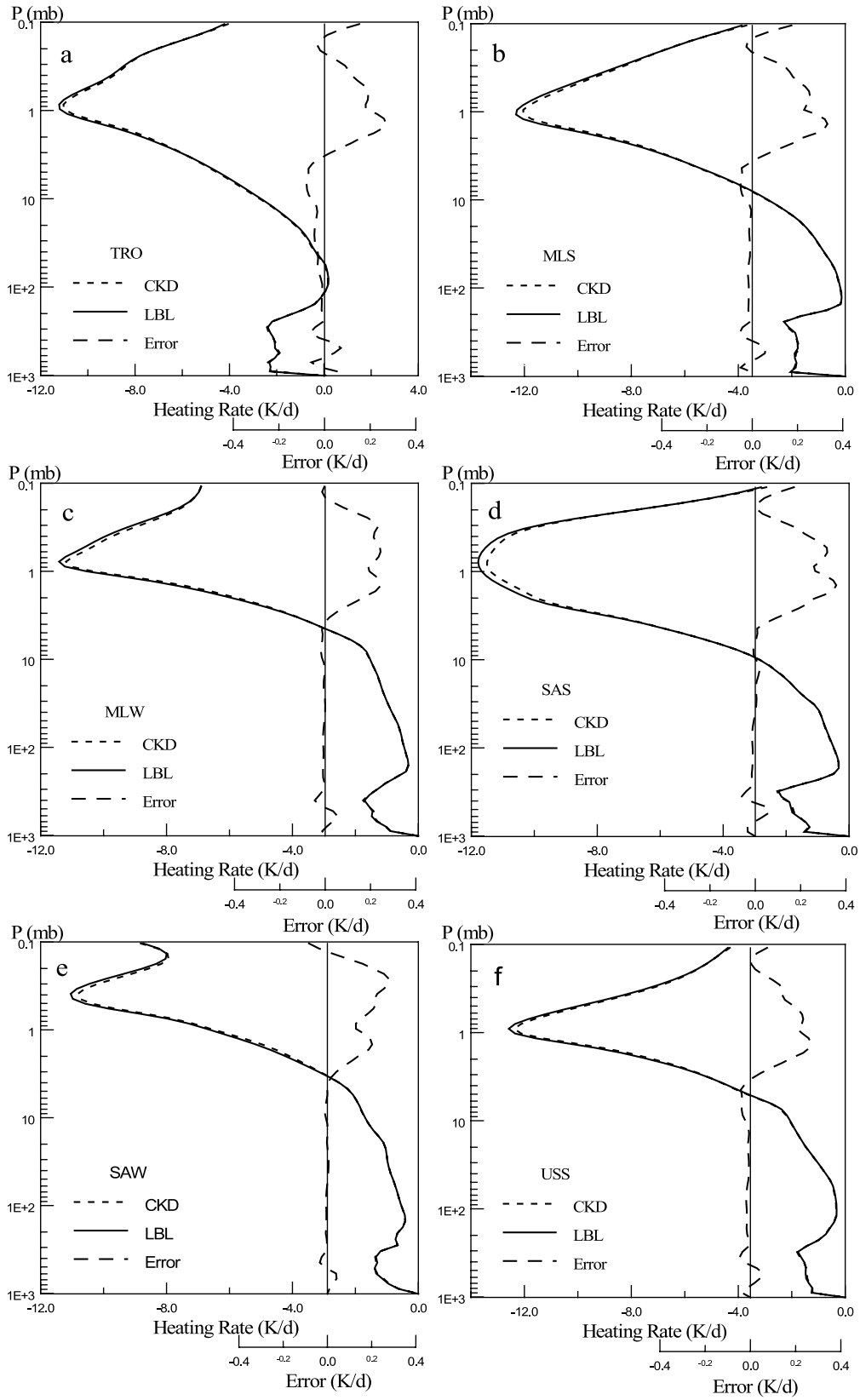

Figure 5. Spectrally integrated longwave heating rates calculated by ck-D model, LBL model, and differences between them for six atmospheres.

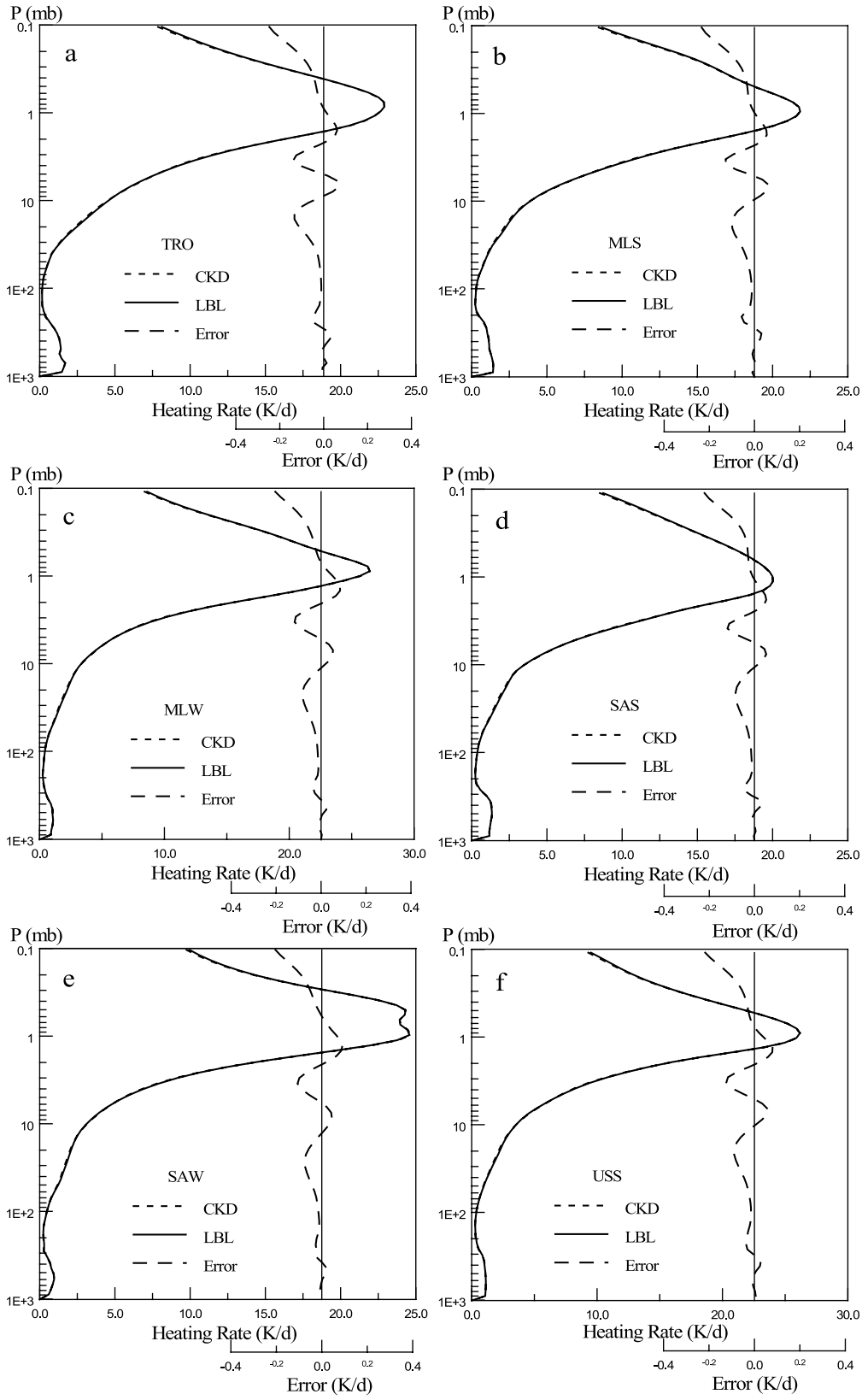

Figure 6. As in Figure 5 but for shortwave heating rates. The surface albedo is 0.2, and the solar zenith angle is 60°.

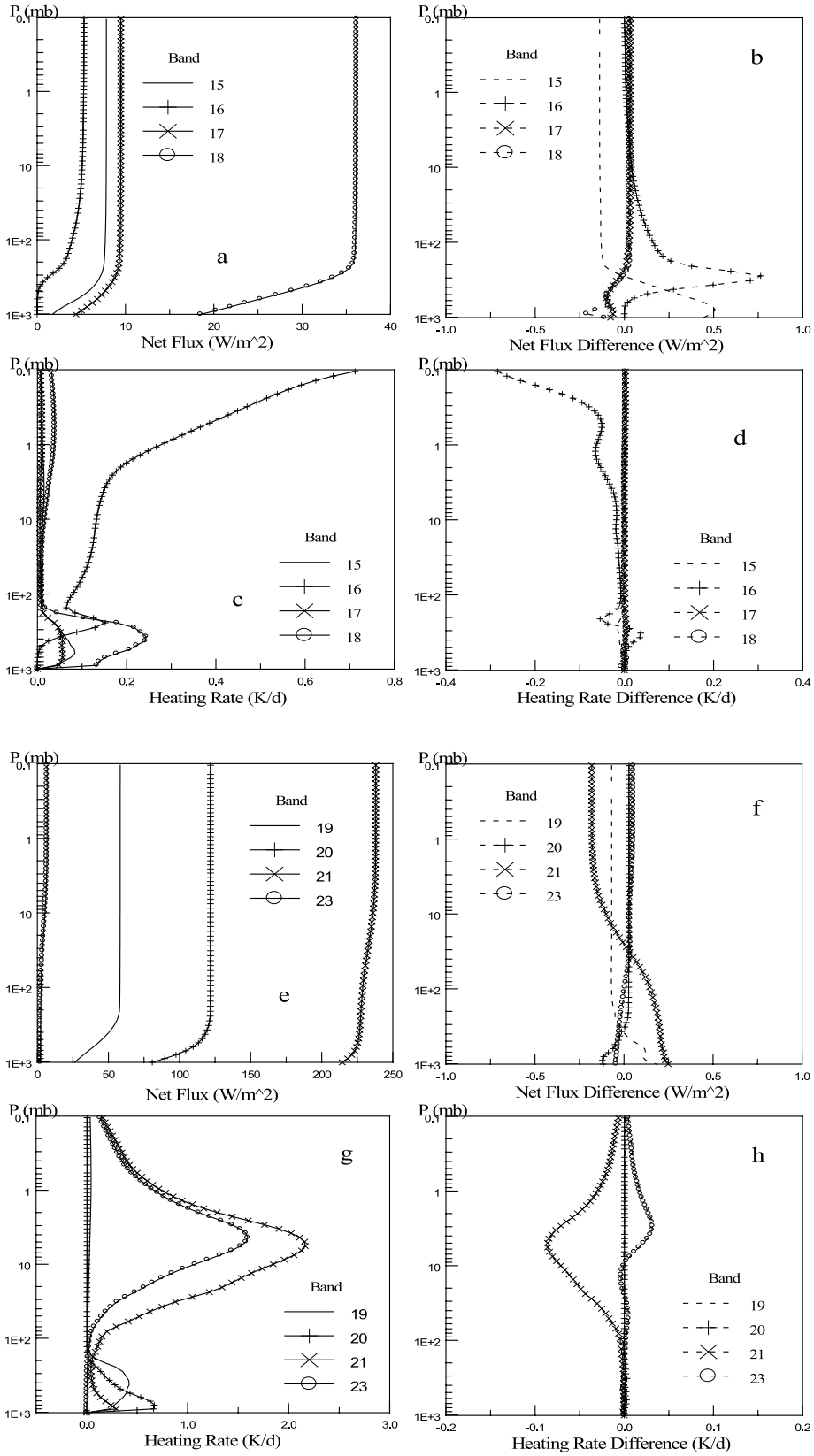

Figure 7. Spectrally integrated net fluxes (a, e, i) and heating rates (c, g, k) for each of the bands 15–27 of shortwave region from 2680 to 49,000 cm^{-1} calculated by LBL model for the MLS atmosphere. Differences between the LBL and ck-D models for these quantities are shown in Figures 7b, 7f, and 7j and in Figures 7d, 7h, and 7l, respectively. The surface albedo is 0.2. The solar zenith angle is 60°.

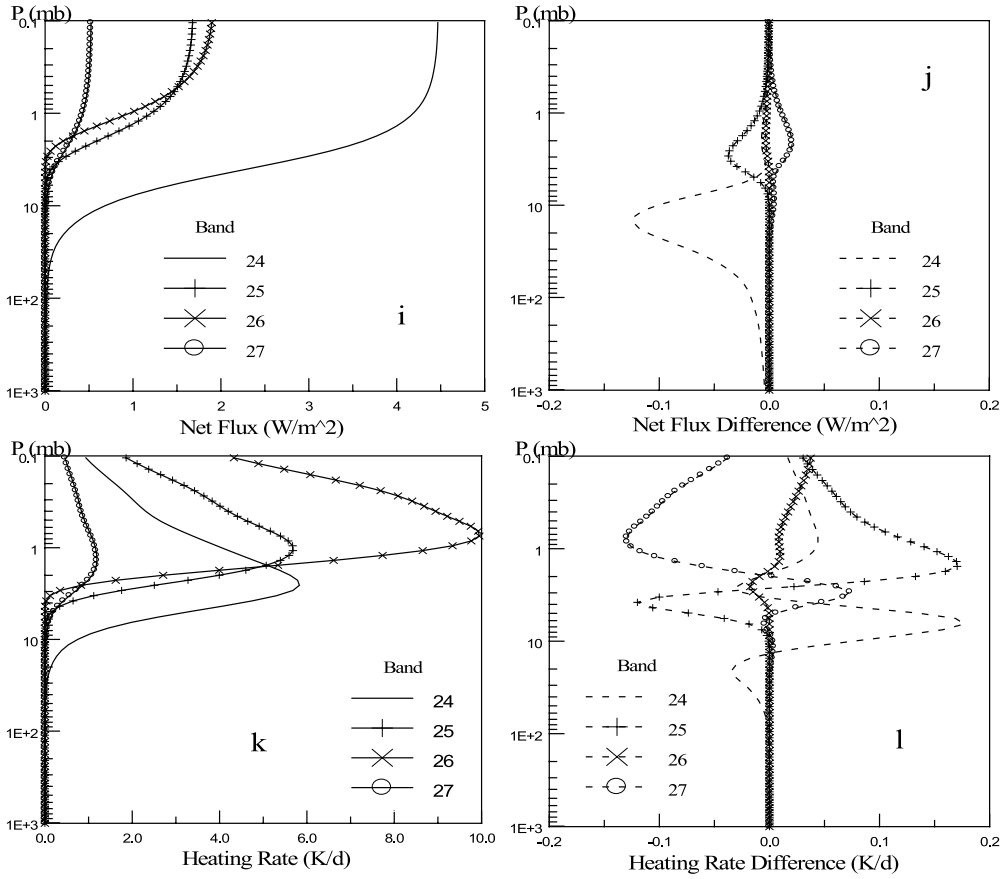

Figure 7. (continued)

As shown in Figure 3, scheme I is related to the partly correlated transmission model described in section 2 that maps the absorption coefficients of minor gas (gas 2 in Figure 3) according to the positions of those of the reference gas (gas 1 in Figure 3) to produce the pale gray line in the figure. Apparently, the line includes the information of correlation of the absorption spectrum to the reference gas. An illustration of scheme II is given in Figure 1; it is related to the completely uncorrelated or perfectly correlated transmission model that resorts the spectrum of minor gas (gas 2 in Figure 1) independently of the reference gas (gas 1 in Figure 1). The k_i values for the minor gas are calculated using two kinds of averages under these two schemes given in Figures 1 and 3. The $k(g)$ in a narrow range near the Gaussian quadrature point under scheme I is averaged to generate k_i^2 in formula (4). All $k(g)$ values in the subinterval under scheme I are averaged to generate k_i^2 in formula (5). Values of $k(g)$ in a narrow range near every Gaussian quadrature point under scheme II are averaged to generate k_j^2 and k_i^2 in formulae (1) and (2).

[21] The k_i values of the water vapor self-continuum are computed separately because of its quadratic dependence on water vapor abundance. The values can be determined by taking an average of all the self-continuum coefficients in each subinterval because of their smooth variation with wave number.

[22] LBL model provides a standard accurate reference for all rapid models, including the algorithms discussed in section 2. The LBL model in this work uses the absorption coefficients calculated directly by LBLRTM to integrate the radiative flux spectrum over wave number. The same radiative transfer scheme adopted in LBL model is also used to calculate the ck-D models to minimize errors beyond that caused by the different wave number integration methods (ck-D versus LBL integration). In this way, the errors between ck-D and LBL models mainly come from different treatments to overlapping bands, and then the validations to the optimal scheme reported here become more effective and objective.

[23] To investigate the accuracy of the algorithms at different pressures, temperatures, and gas concentrations, calculations were performed in detail using six atmospheres from the U.S. Air Force Geophysics Laboratory (AFGL) atmospheric models. The atmospheres included tropical (TRO), MLS, midlatitude winter (MLW), subarctic summer (SAS), subarctic winter (SAW), and U.S. standard (USS) atmospheres under clear-sky conditions. Each atmosphere is divided into 75 homogenous sublayers with 1-km resolution. The thermal and solar radiation transfer calculation is solved with the same scheme as that of *Lacis and Oinas* [1991] to treat vertical inhomogeneity in each sublayer with a modified diffusivity factor approximation [*Zhang and Shi*, 2001] and a two-stream algorithm developed by *Nakajima et al.* [2000]. It should be noted that the radiative net flux is defined as the upward flux minus downward flux at longwave and as the downward flux

minus upward flux at shortwave throughout the whole calculation in this paper.

4. Validation

[24] Table 1 presents the spectral bands of the ck-D methods in longwave and shortwave regions, including gas species, *k*-interval numbers, and transmittance schemes for each band. The spectral region is divided into 27 bands: 14 bands in the longwave region and 13 bands in the shortwave region. This band division is used throughout this work. Surface reflectance is fixed at 0.2 and solar zenith angle is fixed at 60° in all the standard calculations, except where noted. The concentration of N_2O and CH_4 is adopted as 0.32 and 1.70 ppmv, respectively; the concentration of CO_2 is taken to be 330 ppmv in this study except for the Table 2 calculation in the following.

4.1. Spectrally Integrated Results

[25] Table 3 gives the comparison of net fluxes at TOA, tropopause, and the surface, which are calculated by the LBL model and the present schemes for six atmospheres, respectively. Maximum errors of the net flux do not exceed 0.7 W m^{-2} for these three typical altitudes and less than 0.9 W m^{-2} at any altitude for the six atmospheres for both longwave and shortwave regions.

[26] Figures 5a–5f show spectrally integrated longwave heating rate calculated by the ck-D model and the LBL model for six atmospheres and the differences between the two models. Note that the error abscissa has a different scale in these figures. Maximum errors are less than 0.07 K d^{-1} for the entire troposphere and 0.35 K d^{-1} above the tropopause for all six atmospheres. Errors are very small between the tropopause (around 11 km) and the middle of the stratosphere (around 40 km). The largest error is less than 0.05 K d^{-1} for MLS, MLW, SAS, SAW, and USS atmospheres and less than 0.07 K d^{-1} for the TRO atmosphere. Band-by-band results are not shown here since similar results have been given by *Mlawer et al.* [1997].

[27] Figure 6 is the same as Figure 5 but for the heating rates in the shortwave. The greatest errors for six atmospheres all lie in the TOA (0.1 mbar). The errors are less than 0.05 K d^{-1} in the troposphere and less than 0.25 K d^{-1} above the tropopause. The band-by-band results in the solar region are shown in Figure 7 for the MLS atmosphere. It shows that the absolute errors of the solar radiative net fluxes at all levels are less than 0.25 W m^{-2} except for band 15 and band 16, which arrive at 0.5 W m^{-2} at the surface and 0.76 W m^{-2} at the altitude of 10 km, respectively, and the absolute errors of the solar heating rates are less than 0.18 K d^{-1} at all the levels except for band 16, which reaches 0.28 K d^{-1} at TOA.

[28] To determine the accuracy of the ck-D method for a more comprehensive set of atmospheric conditions a climate model will see, we perform our validations here based on an ensemble of 42 diverse profiles taken from the work of *Garand et al.* [2001]. The first 6 in these 42 profiles are standard profiles that are the same as those described above, the 12 profiles of 7–18 are ranked by increasing mean (mass weighted) atmospheric temperature, the next 12 (19–30) are ranked by increasing integrated water vapor, and the last 12 (31–42) by increasing total ozone. Figures 8a and 8b give the maximum errors between the ck-D and LBL longwave heating rate for each of these 42 profiles in and above tropopause, respectively. It gives that the average value of these maximum heating rate errors is 0.068 K d^{-1} in troposphere and 0.22 K d^{-1} above tropopause for the 42 profiles. The accuracy of radiative net flux is 1.1 W m^{-2} at all levels for these profiles. (Figure is ignored here.)

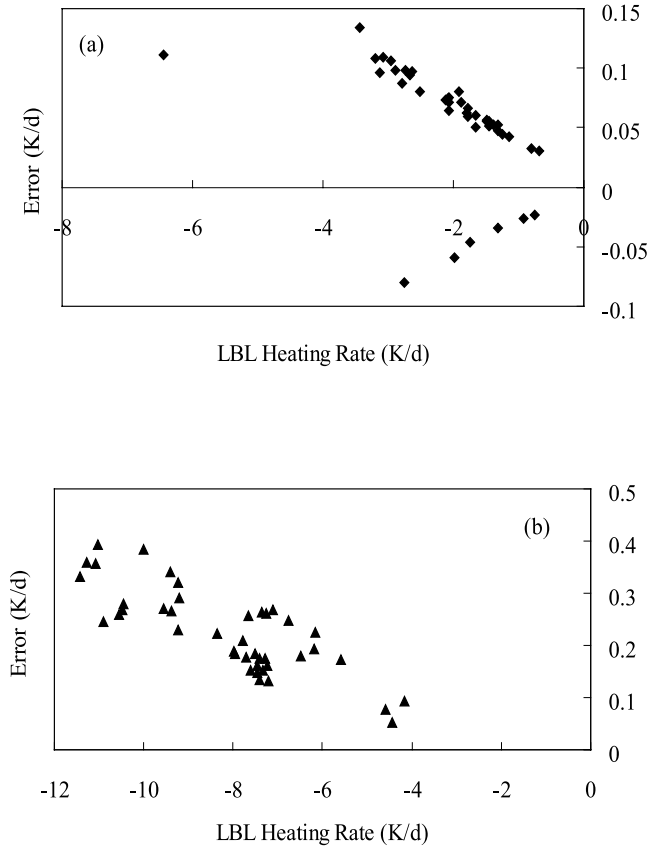

Figure 8. Maximum longwave heating rate errors for each of the 42 atmospheric profiles at (a) troposphere and at (b) stratosphere and middle atmosphere.

4.2. Sensitivity to Doubling CO_2

[29] The set of k_i parameters in the ck-D model is derived with a CO_2 concentration of 330 ppmv. However, the radiative flux and heating rate from the ck-D method are consistent with those of the LBL model in a doubled CO_2 case. Figures 9a and 9b show spectrally integrated upward, downward, and net fluxes, and the differences between the ck-D model and the LBL model at a CO_2 concentration of 660 ppmv for the MLS atmosphere. Errors in the fluxes are less than 0.9 W m^{-2} for the whole atmosphere. Figure 9c compares the heating rates from the LBL and models for the doubled CO_2 case. A maximum error is 0.06 K d^{-1} near the surface and increases to 0.45 K d^{-1} at heights around 50 km. This is similar to the case with present-day CO_2 concentrations (330 ppmv), for which case errors range from 0.059 to 0.33 K d^{-1}. Results from ck-D model are consistent with LBL model over a range of CO_2 concentrations.

[30] Table 2 shows the flux errors for CO_2 concentration doubled from the current level of 355 ppmv. Three hundred

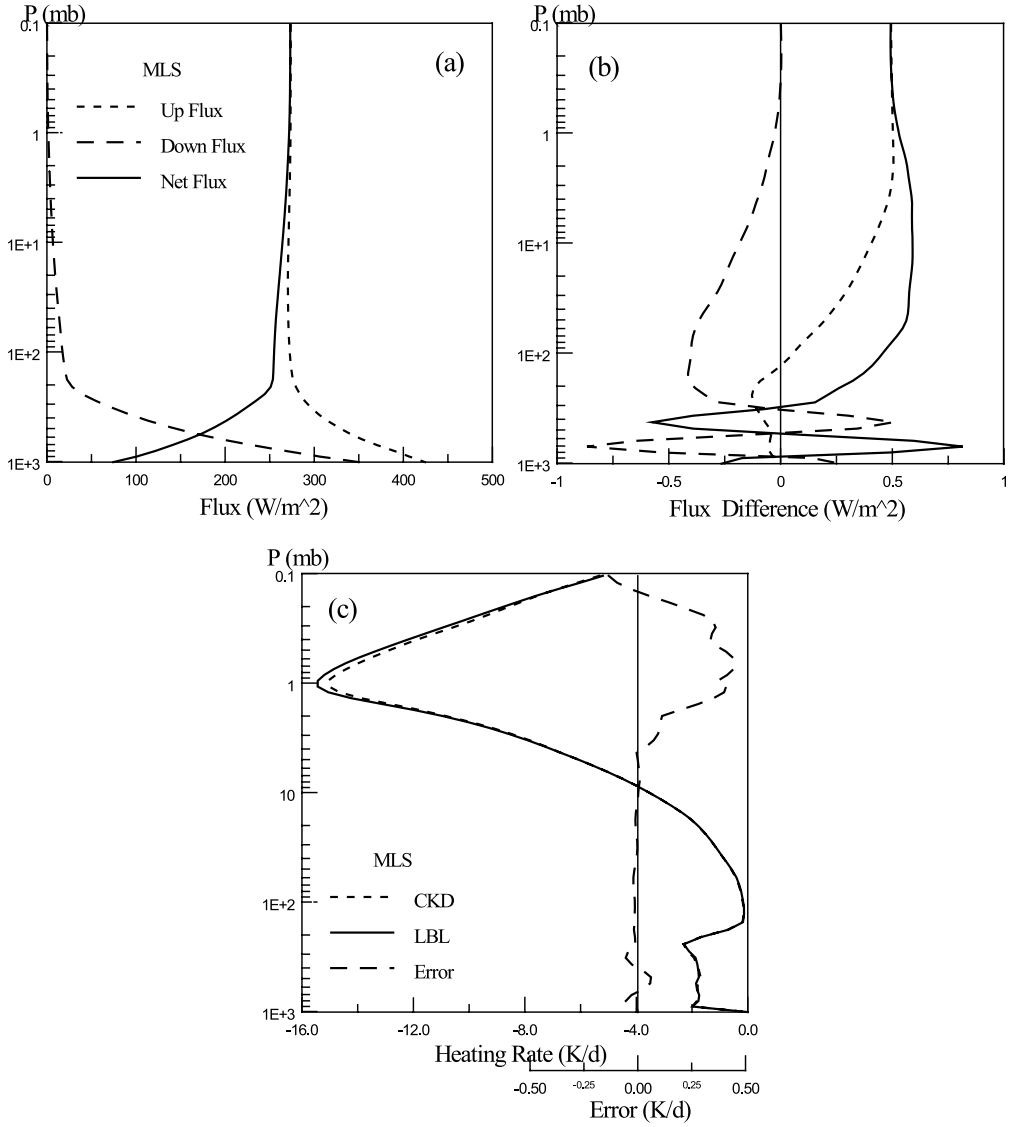

Figure 9. (a) Spectrally integrated longwave upward, downward, and net fluxes calculated by LBL model for MLS atmosphere for doubled CO_2 case and (b) differences in these fluxes between LBL and ck-D model. (c) Spectrally integrated heating rates calculated by LBL model (solid line) and ck-D model (short dashed line) and errors between them (long dashed line).

and fifty-five ppmv of CO_2 concentration adopted here is to be the same as that of LBLRTM. The accuracies of net flux of the LBL model and the ck-D model, found by comparison with corresponding values from the LBLRTM (see column error 2), are 0.39 and 0.35 W m^{-2}, respectively. It demonstrates that the results of this work are consistent with LBLRTM, even though there exist many different factors in the calculations. Note that the reference values of LBLRTM in Table 2 are taken from the work of *Mlawer et al.* [1997], and there exist some differences between different versions of LBLRTM used by *Mlawer et al.* [1997] and in this study (S. A. Clough et al., 2000, available at http://www.rtweb.aer.com). For example, different versions of the HITRAN database are used since we use the updated HITRAN'2000 as an input when running LBLRTM (HITRAN'2000 here versus HITRAN'1992), different continuum models (CKD_2.4 in the present model versus CKD_2.1), and different radiative transfer schemes. In addition, Table 2 also shows that the accuracy of the radiative forcing for the doubled CO_2 concentration is 0.04 W m^{-2}, which is indicated by the net flux difference at the tropopause in Table 2.

5. Summary

[31] An efficient approach to solve overlapping band absorption using the ck-D method, which is especially suitable for wide band absorption, is presented in this paper. The k distribution parameters of species in each band are calculated using an optimized rule dependent on correlations. For six model atmospheres, accuracy in this study is 0.07 K d^{-1} for the heating rate for longwave clear-sky radiation for the entire troposphere and 0.35 K d^{-1} above the tropopause; the accuracy of upward, downward, and net fluxes is 0.76 W m^{-2} at all altitudes. For shortwave regime, the absolute heating rate error is less than 0.05 K d^{-1} in the troposphere and 0.25 K d^{-1} above the tropopause. Net flux

errors are less than 0.9 W m^{-2} at any altitude. For a representative set of 42 atmospheric profiles, it shows that an average error of maximum heating rate is 0.068 K d^{-1} in troposphere and 0.22 K d^{-1} above tropopause; the accuracy of radiative net flux is 1.1 W m^{-2} at all levels. Radiative forcing due to doubled CO_2 concentration has a higher accuracy of 0.04 W m^{-2}.

[32] The overlapping approach with the ck-D model presented here has the following features. (1) It treats the overlapping bands efficiently and thus makes a fast radiation computation due to using an optimal transmission model related to the real correlation between overlapping gases and not using solely the most time-consuming multiplication transmission model. (2) It allows any number of species, including halocarbons, in each band to overlap. (3) The *k* distribution parameters themselves do not include any information related to absorber amount and thus are generally applicable to the full set of atmospheric conditions with a higher accuracy, as reported in this paper.

[33] The purpose of this paper is to provide an optimal and effective method to treat overlapping bands in atmospheric absorption. It is proved that the new scheme is effective not only for broadband from several tens to several hundreds of wave numbers but also for very narrow bandwidths like 5 cm^{-1}. However, the radiative scheme devised in the paper, including the band division and the choice of subinterval number in each band, is not necessarily appropriate to be used in climate model directly at present because of possibly speedy problem. We need to take a further test and then make a balance between speed and accuracy when applying in future climate modeling.

[34] **Acknowledgments.** The authors are grateful to T. Kimura, Y. Tsushima, and M. Sekiguchi for the beneficial discussions in some calculation of this study and are also thankful to W. O. Gallery, S. A. Clough, and R. G. Ellingson for their help during running LBLRTM. This work is supported partly by the Bureau of Resource and Environment, CAS (contract KZCX2-305 and KZCX2-SW-210), and the 973 Project of the MOST (contract G2000048703).

References

Buchwitz, M., V. V. Rozanov, and J. P. Burrows, A correlated-*k* distribution scheme for overlapping gases suitable for retrieval of atmospheric constituents from moderate resolution radiance measurements in the visible/near-infrared spectral region, *J. Geophys. Res.*, *105*, 15,247–15,261, 2000.

Chou, M.-D., Atmospheric solar heating in minor absorption bands, *Terr. Atmos. Ocean Sci.*, *10*, 511–528, 1999.

Chou, M.-D., X.-Z. Liang, and M. M.-H. Yan, Technical report series on global modeling and data assimilation, *Rep. TM-10,4606*, vol. 19, pp. 8–15, NASA, Greenbelt, Md., 2001.

Clough, S. A., and M. J. Iacono, Line-by-line calculation of atmospheric fluxes and cooling rates: 2. Application to carbon dioxide, ozone, methane, nitrous oxide, and the halocarbons, *J. Geophys. Res.*, *100*, 16,519–16,535, 1995.

Clough, S. A., M. J. Iacono, and J.-L. Moncet, Line-by-line calculations of atmospheric fluxes and cooling rates: Application to water vapor, *J. Geophys. Res.*, *97*, 15,761–15,785, 1992.

Ellingson, R. G., J. Ellis, and S. Fels, Intercomparison of radiation codes used in climate models: Longwave results, *J. Geophys. Res.*, *96*, 8929–8953, 1991.

Firsov, K. M., A. A. Mitsel, Y. N. Ponomarev, and I. V. Ptashnik, Parameterization of transmittance for application in atmospheric optics, *J. Quant. Spectrosc. Radiat. Transfer*, *59*, 203–213, 1998.

Fu, Q., and K.-N. Liou, On the correlated *k* distribution method for radiative transfer in nonhomogeneous atmospheres, *J. Atmos. Sci.*, *49*, 2139–2156, 1992.

Garand, L., et al., Radiance and Jacobian intercomparison of radiative transfer models applied to HIRS and AMSU channels, *J. Geophys. Res.*, *106*, 24,017–24,031, 2001.

Gerstell, M. F., Obtaining the cumulative *k*-distribution of a gas mixture from those of its components, *J. Quant. Spectrosc. Radiat. Transfer*, *49*, 15–38, 1993.

Goody, R. M., R. West, L. Chen, and D. Crisp, The correlated-*k* methods for radiation calculations in nonhomogeneous atmospheres, *J. Quant. Spectrosc. Radiat. Transfer*, *42*, 539–550, 1989.

Isaacs, R. G., W.-C. Wang, R. D. Worsham, and S. Goldenberg, Multiple scattering LOWTRAN and FASCODE models, *Appl. Opt.*, *26*, 1272–1281, 1987.

Lacis, A. A., and V. Oinas, A description of the correlated *k* distribution method for modeling nongray gaseous absorption, thermal emission, and multiple scattering in vertically inhomogeneous atmospheres, *J. Geophys. Res.*, *96*, 9027–9063, 1991.

Liu, F., G. J. Smallwood, and Ö. L. Gülder, Application of the statistical narrow-band correlated-*k* method to non-grey gas radiation in CO_2-H_2O mixtures: Approximate treatments of overlapping bands, *J. Quant. Spectrosc. Radiat. Transfer*, *68*, 401–417, 2001.

Mlawer, E. J., S. J. Taubman, P. D. Brown, M. J. Iacono, and S. A. Clough, Radiative transfer for inhomogeneous atmospheres: RRTM, a validated correlated-*k* model for the longwave, *J. Geophys. Res.*, *102*, 16,663–16,682, 1997.

Nakajima, T., M. Tsukamoto, Y. Tsushima, A. Numaguti, and T. Kimura, Modeling of the radiative process in an atmospheric general circulation model, *Appl. Opt.*, *39*, 4869–4878, 2000.

Shi, G.-Y., An accurate calculation and representation of the infrared transmission function of the atmospheric constituents, Ph.D. thesis, Tohoku Univ. of Jpn., Sendai, Japan, 1981.

Shi, G.-Y., Effect of atmospheric overlapping bands and their treatment on the calculation of thermal radiation, *Chin. Adv. Atmos. Sci.*, *1*, 246–255, 1984.

Shi, G.-Y., On correlated *k* distribution model in radiative calculation, *Chin. J. Atmos. Sci.*, *22*, 659–676, 1998.

Wang, W.-C., and P. B. Ryan, Overlapping effect of atmospheric H_2O, CO_2 and O_3 on the CO_2 radiative effect, *Tellus, Ser. B*, *35*, 81–91, 1983.

Yang, S.-R., P. Ricchiazzi, and C. Gautier, Modified correlated *k*-distribution methods for remote sensing applications, *J. Quant. Spectrosc. Radiat. Transfer*, *64*, 585–608, 2000.

Zhang, H., On the study of a new correlated *k* distribution method for nongray gaseous absorption in the inhomogeneous scattering atmosphere, Ph.D. thesis, Inst. of Atmos. Phys., Beijing, 1999.

Zhang, H., and G.-Y. Shi, An improved approach to diffuse radiation, *J. Quant. Spectrosc. Radiat. Transfer*, *70*, 367–372, 2001.

Zhang, H., and G.-Y. Shi, Numerical explanation for accurate radiative cooling rates resulting from the correlated *k* distribution hypothesis, *J. Quant. Spectrosc. Radiat. Transfer*, *74*, 299–306, 2002.

R. Imasu and T. Nakajima, Center for Climate System Research, University of Tokyo, 4-6-1 Komaba, Meguro-ku, Tokyo 153-8904, Japan. (imasu@ccsr.u-tokyo.ac.jp; teruyuki@ccsr.u-tokyo.ac.jp)

G. Shi, State Key Laboratory of Numerical Modeling for Atmospheric Sciences and Geophysical Fluid Dynamics, Institute of Atmospheric Physics, Chinese Academy of Sciences, Beijing 100029, China. (shigy@mail.iap.ac.cn)

T. Suzuki, Integrated Modeling Research Program, Frontier Research System for Global Change, 3173-25 Showamachi, Kanazawa-ku, Yokohama City, Kanagawa 236-0001, Japan. (tsuneaki@jamstec.go.jp)

H. Zhang, Dynamical Climate Division, National Climate Center, China Meteorological Administration, No. 46, Zhong Guan Cun Nan Da Jie, Hai Dian District, Beijing 100081, China. (huazhang@cma.gov.cn)